



ELSEVIER

Contents lists available at ScienceDirect

Applied Catalysis B: Environmental

journal homepage: www.elsevier.com/locate/apcatb



A novel thiocarbamide functionalized graphene oxide supported bimetallic monodisperse Rh-Pt nanoparticles (RhPt/TC@GO NPs) for Knoevenagel condensation of aryl aldehydes together with malononitrile

Betül Şen^{a,1}, Esma Hazal Akdere^{b,1}, Aysun Şavk^a, Emine Gültekin^b, Özge Paralı^a, Haydar Göksu^{b,*}, Fatih Şen^{a,*}

^a Sen Research Group, Biochemistry Department, Faculty of Arts and Science, Dumlupınar University, Evliya Çelebi Campus, 43100 Kütahya, Turkey

^b Kaynaslı Vocational College, Düzce University, Düzce 81900, Turkey

ARTICLE INFO

Keywords:

Knoevenagel condensation
Monodispersity
Novel graphene oxide
RhPt/TC@GO NPs
Thiocarbamide functionalization

ABSTRACT

Functionalization of the graphene provides various possibilities to improve the use of the graphene and to provide more chemical conversion to the graphene. In order to enhance its chemical and physical properties, the graphite which is mainly functionalized with heteroatom-based functional groups is followed intensively, but often results in the inoculation of heteroatoms as various functional groups. Here we show that the graphene oxide can be mainly functionalized with a single species of sulfur and can be reduced to form a graphene which is functionalized with monothiol at the same time. By the help of thiocarbamide-functionalized graphene oxide (TC@GO) the monodisperse rhodium/platinum nanoparticles (RhPt/TC@GO NPs) have been synthesized as promising catalysts for the Knoevenagel condensation to benzylidenemalononitrile derivatives of aryl aldehydes. The monodisperse RhPt/TC@GO NPs have been prepared via a facile method. The novel thiocarbamide-functionalized graphene oxide (TC@GO) supported rhodium/platinum nanoparticles (RhPt/TC@GO NPs) are identified by characterization techniques such as the Raman spectroscopy, high resolution transmission electron microscopy (HRTEM), transmission electron microscopy (TEM), X-ray diffraction (XRD) and X-ray photoelectron spectroscopy (XPS). The spectroscopic and morphological studies of the monodisperse RhPt/TNM@GO NPs indicate the highly crystalline form, well dispersity, ultrafine structure and colloidal stable NPs. After fully characterization of prepared nanoparticles, the novel nanocatalysts have been tried for the Knoevenagel condensation to benzylidenemalononitrile derivatives of aryl aldehydes and show excellent catalytic activity and a yield over 99% by the reaction at room temperature within 8–35 min in the presence of malononitrile and derivatives of aldehyde. As a result, the prepared nanocomposites exhibit very good heterogeneous catalyst properties for Knoevenagel condensation reactions.

1. Introduction

Benzylidenemalononitrile (BMN) derivatives are valuable organic intermediates for the generation of many biologically important molecules such as enzyme inhibitors, carbohydrates and heterocycles [1–5]. On the other hand, both active two CN groups and the presence of double bonds (aliphatic and aromatic) demonstrate the importance of BMN derivatives in organic synthesis [1]. BMN derivatives exhibit various optical, electrical and biological behaviors such as photoluminescence, cyclic-voltammetry, tyrosine kinase enzyme inhibitor properties. These BMN derivatives are shown in Scheme 1 [6–8].

A variety of promising employments have been reported for the

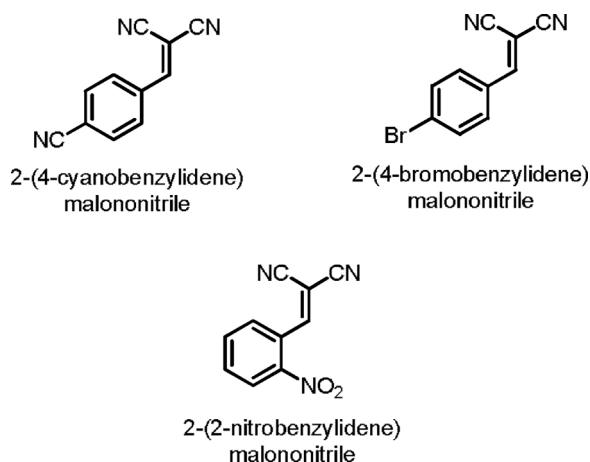
conversion of various aryl bezaldehydes to BMN derivatives, for examples, Cd(II)-based coordination polymer [9], Ni(II)-based coordination polymer [10], MOF (Metal-Organic Framework)-NH₂ [11,12] MOF-Pd [13] PMOV1 [14] PdAlO(OH) [15] Chitosan [16]. However, these commonly used syntheses employ drastic reaction conditions such as high temperature, longer reaction time, poor selectivity and tedious work-up procedures. Over the past decades, increasing scientific and public attention has been focused on heterogeneous catalysts for synthesis of BMN derivatives because they are accessible, reusable, recyclable and they can be easily removed from the reaction medium [17,18].

In recent days, heterogeneous catalysts have been used in various

* Corresponding authors.

E-mail addresses: haydargöksu@duzce.edu.tr (H. Göksu), fatih.sen@dpu.edu.tr (F. Şen).

¹ These authors equally contributed to this work.



Scheme 1. Some optical and biological active BMN derivatives.

organic reactions because they can be easily removed from the mixture and utilized repeatedly. Moreover, the catalytic efficiency and surface area can be increased by reducing the particle size [19–21]. Nowadays, active transition metals nanoparticles have been prepared for using as a catalyst in reactions via variety methods such as conventional, microwave and ultrasonic techniques [22,23]. There has recently been an increased interest in the use of two metal containing nanoparticles (bimetallic) besides single metal containing (monometallic) nanoparticles as heterogeneous catalysts [24–30]. Bimetallic catalysts have been utilized to elucidate the effect on the catalytic activity due to the synergistic effect using activity, better selectivity and stability. Moreover, graphene oxide derivatives (GOD) as support materials provides a better catalytic activity, high surface area and high catalytic stability [22,23,25]. While amine-functionalized GODs are widely pursued, the synthesis of sulfur-functionalized GODs by the wet chemistry method lacks investigations. In this case, we specifically refer only to functionalization in which the nitrogen and sulfur elements are covalently attached to the GODs. In earlier studies, Jonnalagadda and coworkers reported the Knoevenagel reactions in the lack of a solvent catalysed by amine modified zirconia and acid activated clay [31–35]. However, they have received improved results using the functionalized graphene oxide. Besides, Rourke and co-workers have recently functionalized graphene oxide with sulfur via epoxide ring-opening [36]. The resulting thiol-saturated graphene oxide was subsequently applied as a nucleophile to synthesize thioether-functionalized graphene oxide. This is, to the best of our knowledge, the only report on well targeted sulfur functionalization on graphene oxide. Herein, we propose a one-pot monothiolation to provide thiol-functionalized graphene (Fig. 1). In this strategy, hydroxyl and epoxide groups were targeted for thiolation. This is achieved by first subjecting graphene oxide to hydrobromic acid to achieve simultaneous reduction and bromination effects on graphene

oxide. Subsequent addition of thiocarbamide followed by hydrolysis with sodium hydroxide gave thiol-functionalized graphene oxide (GO-SH).

Herein, by the help of thiocarbamide-functionalized graphene oxide (TC@GO) the monodisperse rhodium/platinum nanoparticles (RhPt/TC@GO NPs) have been synthesized as promising catalysts for the Knoevenagel condensation to benzylidenemalononitrile derivatives of aryl aldehydes. These nanocatalyst have been exhibited a simple and facile method for the synthesis of BMN derivatives for the first time. Various aryl benzaldehyde derivatives were easily converted to BMN derivatives in presence of malononitrile in a short period of time with high yields in minimum amount of water.

2. Material and methods

2.1. Preparation of RhPt/TC@GO NPs

The modified Hummers' method was applied to produce graphene oxide from graphite. Briefly, the GO (50 mg) was dispersed in THF (10 mL) in round-bottom flask followed by the addition of Thiocarbamide (TC) (1 mg/mL). It was then stirred for 1 h at room temperature and after that ultrasonicated for 1 h. The mixture was filtrated to separate of dark brown material from solution and washed with EtOH to clean up the final product and was dried in a vacuum oven at 50 °C for 24 h. The sonication method was employed to combine of 30 mg GO-TC, PtCl₄ and RhCl₂ (0.25% w/v) in the mixture with 30 mL of deionized water, and followed by vigorous stirring at 55 °C for 12 h. Afterward, every 5 min 100 µL of NaBH₄ solution was injected to solution and after that repeatedly washed with deionized water. RhPt/TC@rGO NPs have been dried in a vacuum chamber. Besides, the general procedure for the Knoevenagel condensation of aryl aldehydes was given in detail in supporting information.

3. Results and discussion

3.1. The characterization of RhPt/TC@GO NPs nanoparticles

The synthesized homogeneously distributed RhPt/TC@GO NPs bimetallic nanoparticles were characterized by XRD as compared to monometallic Pt and Rh nanoparticles. XRD models of Pt@GO and Rh@GO monometallic and Rh-Pt@GO bimetallic nanoparticles are shown in Fig. 1. For the Pt nanoparticles in the monometallic structure, there are four characteristic diffraction peaks of the fcc structure which correspond to the (111), (200), (220) and (311) planes, respectively. Four peaks are also clearly visible for the Pt@GO monometallic structure and RhPt/TC@GO NPs bimetallic structure. RhPt/TC@GO NPs bimetallic nanoparticles showed the strong diffraction peaks corresponding to the Pt and Rh alloy. As shown in Fig. 1a, there is a slightly shift compared to the monometallic one which indicates the alloy formation of RhPt. That's why we thought that Pt formed the same alloy as

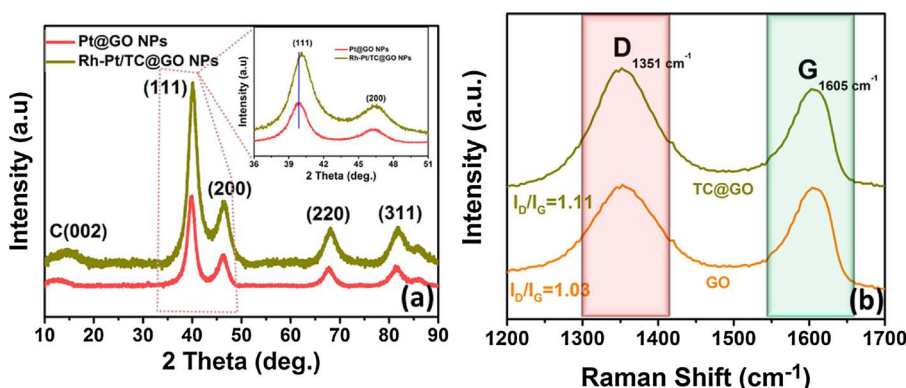


Fig. 1. (a) XRD pattern of RhPt/TC@GO NPs (b) Raman spectra of GO and TC@GO.

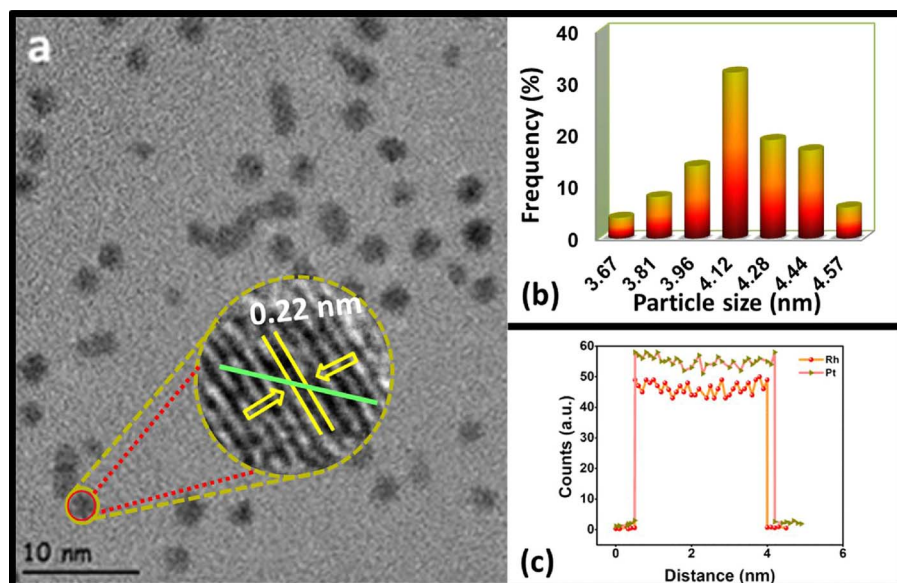


Fig. 2. (a) TEM image, (b) particle size histogram, (c) EELS line profile RhPt/TC@GO NPs.

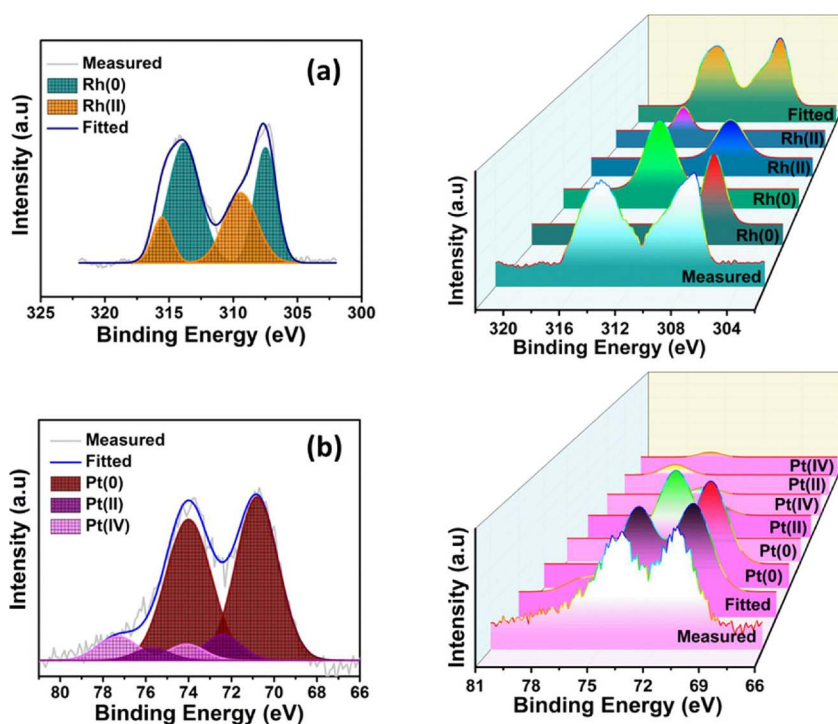


Fig. 3. XPS spectra (a) Pt 4f region and (b) Rh 3d region of RhPt/TC@GO NPs.

Rh during the reduction process. The average crystalline particle size of RhPt/TC@GO NPs was calculated by the help of Scherrer equation. The average crystalline particle size of the RhPt/TC@GO NPs was found to be 3.64 nm as a result of the calculation. [37–39]. Further analyses with Raman spectroscopy on GO and TC@GO showed obvious D (breathing mode of sp²-hybridized carbon) and G (graphitic sp²-hybridized carbon) bands, as seen in Fig. 1b. The ratio of peak intensities for D and G bands (ID/IG) reflects the extent of defects on graphene materials, in which GO and TC@GO showed values of 1.03 and 1.11, respectively. The slightly higher extent of defects (D/G ratio) on TC@GO is common for GO materials that have undergone reduction or functionalization treatments.

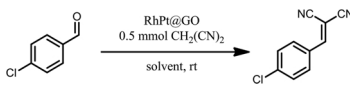
The monodisperse RhPt/TC@GO NPs were also been analyzed by TEM and HR-TEM for particle size distribution and morphology of the structure. As can be seen from the TEM picture, the fine particles are distributed homogeneously with the aid of thiocarbamide-

functionalized graphene oxide support (Fig. 2a). In addition, an HR-TEM was used to analyze atomic lattice fringe of monodisperse RhPt/TC@GO NPs. As an effect of these fringes, RhPt (111) plane was observed with a fringe of 0.22 nm on the prepared nanocatalyst; which is a bit smaller than the 0.23 nm of Pt nominal value [25,39,40]. This case also indicates the alloy formation of RhPt/TC@GO NPs. A particle size histogram was made for a size distribution of the prepared nanocomposites in which 100 particles were targeted. As a result, it is seen that the distribution is Gaussian and the most reasonable size of the particles is around 4.12 ± 0.45 nm (Fig. 2b). Furthermore, EELS line profile of RhPt/TC@GO NPs indicates also the existence of both Rh and Pt in the structure which shows the alloy formation of NPs. Besides, when we compare the particle sizes obtained from the XRD and TEM results, we can see that the results are in good agreement with each other.

When the XPS spectrum of RhPt/TC@GO NPs bimetallic

Table 1

Optimization experiments for Knoevenagel condensation of 4-chlorobenzaldehyde with malononitrile.^a

				
Entry	Solvent	Catalyst (mg)	Time (min)	Yield ^b (%)
1	CH ₂ Cl ₂	2	120	Trace
2	CH ₃ CN	2	120	Trace
3	EtOH	2	120	15
4	MeOH	2	120	55
5	IPA	2	120	15
6	H ₂ O	2	120	28
7	H ₂ O/MeOH (1:1)	2	20	90
8	H ₂ O/MeOH (2:1)	2	30	82
9	H ₂ O/MeOH (1:2)	2	8	> 99
10	H ₂ O/MeOH (1:2)	–	240	Trace

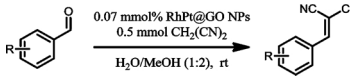
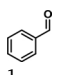
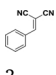
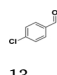
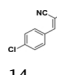
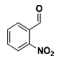
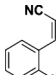
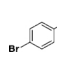
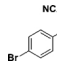
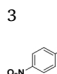
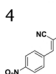
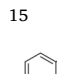
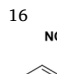

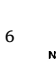
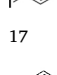
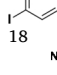
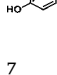
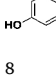
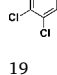
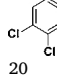
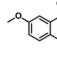
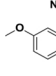
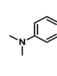
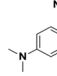
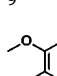
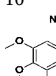
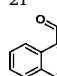
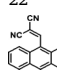
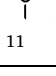
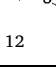


^a Reaction conditions: 4-chlorobenzaldehyde (0.25 mmol), malononitrile (0.5 mmol), RhPt@GO NPs (%10.8 wt metal content) and room temperature.

^b GC yield.

nanocomposites in Pt 4f and Rh 3d regions were examined, the results were shown in Fig. 3a and b. As shown from these figures, the Pt 4f spectrum shows a doublet that consists of a high energy band (Pt 4f_{5/2}) at 70.1 eV and a low energy band (Pt 4f_{7/2}) at 74.3 eV, and the Rh 3d spectrum shows a doublet that consists of a high energy band (Rh 3d_{3/2}) at 313.4 eV and a low energy band (Rh 3d_{5/2}) at 307.1 eV, indicating the existence of metallic Pt and Rh.

Table 2

Knoevenagel condensation reaction in the presence of RhPt/TC@GO NPs catalyst between aryl aldehyde derivatives and malononitrile structure.^a

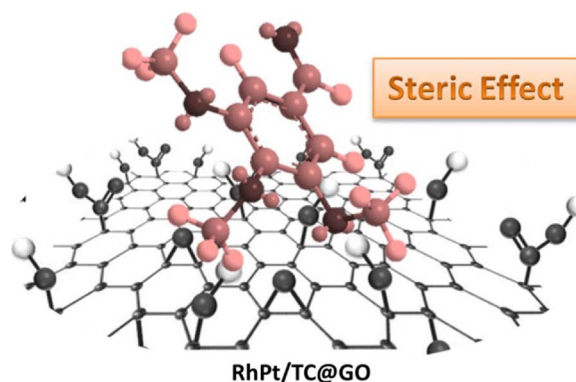
									
Entry	Substrate	Product	Con ^b /Sel ^c /Yield ^d %	Time (min)	Entry	Substrate	Product	Con ^b /Sel ^c /Yield ^d %	Time (min)
1			> 99/100/ > 99	10	7			> 99/100/ > 99	8
2			> 99/100/ > 99	8	8			> 99/100/ > 99	10
3			> 99/100/ > 99	8	9			> 99/100/ > 99	20
4			> 99/100/ > 99	15	10			> 99/100/ > 99	10
5			> 99/100/ > 99	16	11			> 99/100/ > 99	30
6			> 99/100/ > 99	20	12			> 85/100/ > 85	35
11					23				
12					24				

^a Reaction conditions: Substrate (0.25 mmol), malononitrile (0.5 mmol) and RhPt/TC@GO NPs (2 mg, %10.8 wt metal content) was used with 1.5 mL of water/methanol (v/v = 1/2) at room temperature.

^b GC conversion based on aromatic substrates.

^c Selectivity based on GC results.

^d GC yield.



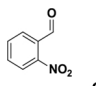
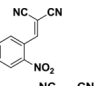
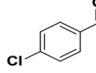
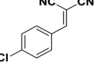
Scheme 2. Proposed approach towards catalyst surface of 3,4,5-trimethoxybenzaldehyde.

Besides, as shown in XPS figures, there is a small amount of higher oxidation state of Pt (+2 and +4) and Rh (+2) in RhPt/TC@GO NPs. These higher oxidation states of Rh and Pt can be explained by the oxidized species of Rh and Pt and/or some of the unreduced species of Rh and Pt.

3.2. Optimization experiments for Knoevenagel condensation of 4-chlorobenzaldehyde with malononitrile in the presence of RhPt/TC@GO NPs

As illustrated in Table 1, the process was tried to optimize by the amount of malononitrile, solvent system and time interval. It was aimed

Table 3
Reusability test of monodisperse RhPt/TC@GO NPs.^a

Entry	Substrate	Product	1st		5th	
			Yield ^b (%)	Time (min)	Yield ^b (%)	Time (min)
1			> 99	8	98	12
2			> 99	8	96	15

^a Reaction conditions: substrate (0.25 mmol), malononitrile (0.5 mmol) and RhPt/TC@GO NPs (2 mg, %10.8 wt metal content), 1.5 mL of water/methanol (v/v = 1/2) and room temperature.

^b GC yield.

Table 4
Comparison of designed catalytic system with recent published works about the Knoevenagel condensation of benzaldehyde with malononitrile.

Catalyst	Solvent	Temp. °C	Time, min	Conv., %	Ref.
MOF-NH ₂ ⁵	DMF	80	270	51	[11]
NH ₂ (50%)-MIL-53 ³	Methanol	80	15	99	[12]
MOF-Pd ⁴	DMSO- <i>d</i> ₆	25	5	42.5	[13]
PMOV1 ¹	Solvent free	70	45	86	[14]
PdAlO(OH) ⁶	Water/methanol (v/v = 1/2)	25	35	85	[15]
Chitosan ²	Ethanol	40	360	> 99	[16]
RhPt/TC @GO NPs	Water/methanol (v/v = 1/2)	25	10	> 99	This Work

to provide absolute benzylidenemalononitrile (BMN) derivatives formation at room temperature. In literature, yield of BMN production was successfully increased when tetrahydrofuran [41] and ethanol [9] were exhibited as solvent system by the help of heat treatment [42]. Our goal was to achieve Knoevenagel condensation reaction in a short time where water was totally used as eco-friendly solvent without any significant loss of yield. Eventually, 1.0 mmol of 4-chlorobenzaldehyde, 2.0 mg of catalyst and 0.5 mmol of malononitrile gave sufficient performance for Knoevenagel condensation of 4-chlorobenzaldehyde with malononitrile with 1.5 mL of water/methanol (v/v = 1/2) (Table 1, entry 9). The desired product appeared in less than about 4 h with no catalyst present. (Table 1, entry 10).

Besides, Table 2 summarized that all of aryl aldehyde derivatives were successfully converted to benzylidenemalononitrile (BMN) derivatives in the presence of RhPt/TC@GO NPs. The BMN derivatives were quantitatively obtained at room temperature in the minimum solvent environment for periods ranging from about 8–35 min. As shown in this table, benzaldehyde (1) was converted to 2-benzylidenemalononitrile (2) with the yields higher than 99% within 10 min (Table 2, entry 1). The ortho and para-nitro benzaldehydes (3 and 5) were respectively converted to 4 and 6 with the yields higher than 99% within 8 min due to the electron withdrawing properties of nitro groups (Table 2, entries 2, 3). Benzaldehyde derivatives containing hydroxy and methoxy groups (7, 9, 11) were converted to benzylidenemalononitrile derivatives for a somewhat longer time. Because they have electron rich rings (entries 4, 5, 6 respectively). Especially for 3,4,5-trimethoxybenzaldehyde (11), the plausible reason is not only the electron-donating effect but also the sterical hinderence of three methoxy groups (Scheme 2). The 13, 15 and 17 were respectively converted to 14, 16 and 18 with yields of more than 99%. Surprisingly, 17 reacted for a longer time due to the radius of the iodine (Table 2, entries 7–9). The 20 was obtained with yields of more than 99% within 10 min (Table 2, entry 10). 21 and 23 were successfully synthesized. But yields were

found to be lower than other aryl aldehydes. In addition, the process took longer than expected to be completed. (Table 2, entries 11, 12).

The reusability of the RhPt/TC@GO NPs was also be examined in Table 3. The catalyst was used five times and loss in the yield can be tolerated as exhibited in Table 3, Figs. S1 and S2. There is no noticeable loss of rhodium and platinum (0.2 and 0.7 ppm leaching to a solution respectively) after five cycles reusability test confirmed by the ICP-OES analyses. Lastly, as shown in Table 4, the performance of RhPt/TC@GO NPs has been compared with the other catalysts in literature for the model reaction and it was found that the RhPt/TC@GO NPs have shown the best performance compared to the others.

4. Conclusions

As a conclusion, thiocarbamide (TC) functionalized graphene has been produced via a one-pot functionalization. Furthermore, by the help of thiocarbamide-functionalized graphene oxide (TC@GO), the monodisperse rhodium/platinum nanoparticles (RhPt/TC@GO NPs) have been synthesized as promising catalysts for the Knoevenagel condensation to benzylidenemalononitrile derivatives of aryl aldehydes. Besides, the current system is a practically environmentally friendly and recyclable synthetic process. This catalytic system has been shown to exhibit the best catalytic performance as compared to other systems in the literature [11–16], while being interesting for synthesis of the corresponding benzylidenemalononitrile derivatives due to its low particle size, high chemical surface area (67.58 m²/g) and high % metal (O) content. Also, the novel prepared catalyst is preferred because it is (i) comparable economical catalyst due to no need for a special system (ii) very efficient and environmentally friendly, (iii) safe, (iv) easy to use in ambient conditions. For this reason, the literature will gain a new perspective on the usage of novel supported heterogeneous catalysts and the irappplication of Knoevenagel condensation. The success of this method provides a simple and scalable one-pot synthesis of TC-functionalized graphene to facilitate future developments of advanced graphene-based applications.

Acknowledgements

This research was supported by Duzce University (grant no. 2015.26.04.371) and Dumlupinar University Research Fund (2014-05, 2016-75 and 2017-40). The partial supports from Science Academy and FABED are highly acknowledged.

Appendix A. Supplementary data

Supplementary data associated with this article can be found, in the online version, at <https://doi.org/10.1016/j.apcatb.2017.11.067>.

References

- [1] M.N. Elinson, S.K. Feducovich, N.O. Stepanov, A.N. Vereshchain, A new strategy of the chemical route to the cyclopropane structure: direct transformation of benzylidenemalononitriles and malononitrile into 1,1,2,2-tetracyanocyclopropanes, *Tetrahedron* 64 (2008) 708–713.
- [2] S.S. Maltsev, M.A. Mironov, V.A. Bakulev, Synthesis of cyclopentene derivatives by the cyclooligomerization of isocyanides with substituted benzylidenemalononitriles, *Mendelev Commun.* 16 (2006) 201–202.
- [3] M.N. Elinson, A.N. Vereshchain, N.O. Stepanov, T.A. Zaimovskaya, V.M. Merkulova, G.I. Nikishin, The first example of the cascade assembly of a spirocyclopropane structure: direct transformation of benzylidenemalononitriles and N,N-dialkylbarbituric acids into substituted 2-aryl-4,6,8-trioxo-5,7-diazaspiro[2.5]octane-1,1-dicarbonitriles, *Tetrahedron Lett.* 51 (2010) 428–431.
- [4] Q. Hu, X.L. Shi, Y. Chen, X. Han, P. Duan, Revisiting the Knoevenagel condensations: a universal and flexible bis-ammoniated fiber catalyst for the mild synthesis of a,b-unsaturated compounds, *J. Ind. Eng. Chem.* 54 (2017) 75–81.
- [5] H. Xu, L. Pan, X. Fang, B. Liu, W. Zhang, M. Lu, Y. Xu, T. Ding, H. Chang, Knoevenagel condensation catalyzed by novel Nmm-based ionic liquids in water, *Tetrahedron Lett.* 58 (2017) 2360–2365.
- [6] K. Turpaev, M. Ermolenko, T. Cresteil, J.C. Drapier, Benzylidenemalononitrile compounds as activators of cell resistance to oxidative stress and modulators of

- multiple signaling pathways. A structure–activity relationship study, *Biochem. Pharm.* 82 (2011) 535–547.
- [7] A. Gazit, P. Yaish, C. Gilon, A. Levitzki, I. Tyrphostin, Synthesis and biological activity of protein tyrosine kinase inhibitors, *J. Med. Chem.* 32 (1989) 2344–2352.
 - [8] A. Levitzki, E. Mishani, Tyrphostins and other tyrosine kinase inhibitors, *Annu. Rev. Biochem.* 75 (2006) 93–109.
 - [9] A. Karmakar, A. Paul, K.T. Mahmudov, M.F.C.G. Silva, A.J.L. Pombeiro, pH dependent synthesis of Zn(ii) and Cd(ii) coordination polymers with dicarboxyl-functionalized arylhydrazones of barbituric acid: photoluminescence properties and catalysts for Knoevenagel condensation, *New J. Chem.* 40 (2016) 1535–1546.
 - [10] R.A. Agarwal, S. Mukherjee, Two-dimensional flexible Ni(II)-based porous coordination polymer showing single-crystal to single-crystal transformation, selective gas adsorption and catalytic properties, *Polyhedron* 105 (2016) 228–237.
 - [11] A. Taher, D.J. Lee, B.K. Lee, I.M. Lee, Amine-functionalized metal-organic frameworks: an efficient and recyclable heterogeneous catalyst for the Knoevenagel condensation reaction, *Synlett* 27 (2016) 1433–1437.
 - [12] F. Martinez, G. Orcajo, D. Briones, P. Leo, G. Calleja, Catalytic advantages of NH_2 -modified MIL-53(Al) materials for Knoevenagel condensation reaction, *Microporous Mesoporous Mater.* 246 (2017) 43–50.
 - [13] C.I. Ezugwu, B. Mousavi, Md. A. Asraf, Z. Luo, F. Verpoort, Post-synthetic modified MOF for Sonogashira cross-coupling and Knoevenagel condensation reactions, *J. Catal.* 344 (2016) 445–454.
 - [14] B. Viswanadham, P. Jhansi, K.V.R. Chary, H.B. Friedrich, S. Singh, Efficient solvent free Knoevenagel condensation over vanadium containing heteropolyacid catalysts, *Catal. Lett.* 146 (2016) 364–372.
 - [15] H. Goksu, E. Gultekin, Pd nanoparticles incarcerated in aluminium oxy-hydroxide: an efficient and recyclable heterogeneous catalyst for selective Knoevenagel condensation, *ChemistrySelect* 2 (2017) 458–463.
 - [16] B. Sakthivel, A. Dhakshinamoorthy, Chitosan as a reusable solid base catalyst for Knoevenagel condensation reaction, *J. Colloid Interface Sci.* 485 (2017) 75–80.
 - [17] P. Sreenivasarao, S. Subham, C. Ajay, P. Bibudha, D. Jyotirmayee, Reduction of organic azides to amines using reusable Fe_3O_4 nanoparticles in aqueous medium, *Catal. Sci. Technol.* 3 (2013) 584–588.
 - [18] F. Tao, M.E. Grass, Y. Zhang, D.R. Butcher, F. Aksoy, S. Aloni, V. Altöe, S. Alayoglu, J.R. Renzas, C.-K. Tsung, Z. Zhu, Z. Liu, M. Salmeron, G.A. Somorjai, Evolution of structure and chemistry of bimetallic nanoparticle catalysts under reaction conditions, *J. Am. Chem. Soc.* 132 (2010) 8697–8703.
 - [19] Z.C. Wang, W. Chen, Z.L. Han, J. Zhu, N. Lu, Y. Yang, D.K. Ma, Y. Chen, S.M. Huang, Pd embedded in porous carbon (Pd@CMK-3) as an active catalyst for Suzuki reactions: accelerating mass transfer to enhance the reaction rate, *Nano Res.* 7 (2014) 1254–1262.
 - [20] Y. Jiang, X. Zhang, X.P. Dai, W. Zhang, Q. Sheng, H.Y. Zhuo, Y. Xiao, H. Wang, Microwave-assisted synthesis of ultrafine Au nanoparticles immobilized on MOF-199 in high loading as efficient catalysts for a three-component coupling reaction, *Nano Res.* 10 (2017) 876–889.
 - [21] Y. Yıldız, R. Ulus, S. Eris, B. Aday, M. Kaya, F. Sen, Functionalized multi-walled carbon nanotubes (f-MWCNT) as highly efficient and reusable heterogeneous catalysts for the synthesis of acridinedione derivatives, *ChemistrySelect* 1 (13) (2016) 3861–3865.
 - [22] B. Aday, H. Pamuk, M. Kaya, F. Sen, Graphene oxide as highly effective and readily recyclable catalyst using for the one-pot synthesis of 1,8-dioxoacridine derivatives, *J. Nanosci. Nanotechnol.* 16 (2016) 6498–6504.
 - [23] E. Erken, I. Esirden, M. Kaya, F. Sen, Monodisperse Pt NPs@rGO as highly efficient and reusable heterogeneous catalyst for the synthesis of 5-substituted 1H-tetrazole derivatives, *Catal. Sci. Technol.* 5 (2015) 4452–4457.
 - [24] J. Xiang, P. Li, H. Chong, L. Feng, F. Fu, Z. Wang, S. Zhang, M. Zhu, Bimetallic Pd-Ni core-shell nanoparticles as effective catalysts for Suzuki reaction, *Nano Res.* 7 (2014) 1337–1343.
 - [25] H. Goksu, Y. Yıldız, B. Çelik, M. Yazici, B. Kilbas, F. Sen, Highly efficient and monodisperse graphene oxide furnished Ru/Pd nanoparticles for the dehalogenation of aryl halides via ammonia borane, *ChemistrySelect* 5 (2016) 953–958.
 - [26] Y. Yıldız, I. Esirden, E. Erken, E. Demir, M. Kaya, F. Sen, Microwave (Mw)-assisted synthesis of 5-substituted 1H-tetrazoles via [3+2] cycloaddition catalyzed by Mw-Pd/Co nanoparticles decorated on multi-walled carbon nanotubes, *ChemistrySelect* 1 (8) (2016) 1695–1701.
 - [27] L. Wang, Y. Yamauchi, Strategic synthesis of trimetallic Au@Pd@Pt core-shell nanoparticles from poly(vinylpyrrolidone)-Based aqueous solution toward highly active electrocatalysts, *Chem. Mater.* 23 (9) (2011) 2457–2465.
 - [28] L. Wang, Y. Nemoto, Y. Yamauchi, Direct synthesis of spatially-controlled Pt-on-Pd bimetallic nanodendrites with superior electrocatalytic activity, *J. Am. Chem. Soc.* 133 (25) (2011) 9674–9677.
 - [29] L. Wang, Y. Yamauchi, Metallic nanocages: synthesis of bimetallic Pt–Pd hollow nanoparticles with dendritic shells by selective chemical etching, *J. Am. Chem. Soc.* 135 (45) (2013) 16762–16765.
 - [30] L. Wang, Y. Yamauchi, Autoprogrammed synthesis of triple-layered Au@Pd@Pt core-shell nanoparticles consisting of a Au@Pd bimetallic core and nanoporous Pt shell, *J. Am. Chem. Soc.* 132 (39) (2010) 13636–13638.
 - [31] K.M. Parida, S. Mallick, P.C. Sahoo, S.K. Rana, A facile method for synthesis of amine-functionalized mesoporous zirconia and its catalytic evaluation in Knoevenagel condensation, *Appl. Catal. A* 381 (2010) 226–232.
 - [32] G.B.B. Varadwaj, S. Rana, K.M. Parida, Amine functionalized K10 montmorillonite: a solid acid–base catalyst for the Knoevenagel condensation reaction, *Dalton Trans.* 42 (2013) 5122–5129.
 - [33] V.S.R. Pullabhotla, A. Rahman, S.B. Jonnalagadda, Selective catalytic Knoevenagel condensation by Ni–SiO₂ supported heterogeneous catalysts: an environmentally benign approach, *Catal. Commun.* 10 (2009) 365–369.
 - [34] M.K. Pillai, S. Singh, S.B. Jonnalagadda, Solvent-free Knoevenagel condensation over cobalt hydroxyapatite, *Synth. Commun.* 41 (24) (2010) 3710–3715.
 - [35] M.K. Pillai, S. Singh, S.B. Jonnalagadda, Solvent-free Knoevenagel condensation over iridium and platinum hydroxyapatites, *Kinet. Catal.* 52 (4) (2011) 536–539.
 - [36] H.R. Thomas, A.J. Marsden, M. Walker, N.R. Wilson, J.P. Rourke, Sulfur-functionalized graphene oxide by epoxide ring-opening, *Angew. Chem. Int. Ed.* 53 (2014) 7613–7618.
 - [37] B. Sen, S. Kuzu, E. Demir, T.O. Okayay, F. Sen, Hydrogen liberation from the dehydrocoupling of dimethylamine-borane at room temperature by using novel and highly monodispersed RuPtNi nanocatalysts decorated with graphene oxide, *Int. J. Hydrogen Energy* 42 (36) (2017) 23299–23306, <http://dx.doi.org/10.1016/j.ijhydene.2017.04.213>.
 - [38] T. Demirci, B. Çelik, Y. Yıldız, S. Eriş, M. Arslan, B. Kilbas, F. Sen, One-pot synthesis of hantzsch dihydropyridines using highly efficient and stable PdRuNi@GO catalyst, *RSC Adv.* 6 (2016) 76948–76956.
 - [39] Y. Yıldız, T.O. Okayay, B. Sen, B. Gezer, S. Kuzu, A. Savk, E. Demir, Z. Dastdelen, F. Sen, Highly monodisperse Pt/Rh nanoparticles confined in the graphene oxide for highly efficient and reusable sorbents for methylene blue removal from aqueous solutions, *ChemistrySelect* 2 (2) (2017) 697–701.
 - [40] Y. Yıldız, S. Kuzu, B. Sen, A. Savk, S. Akocak, F. Sen, Different ligand based monodispersed Pt nanoparticles decorated with rGO as highly active and reusable catalysts for the methanol oxidation, *Int. J. Hydrogen Energy* (2017) 13061–13069.
 - [41] H. Wang, L. Li, X.F. Bai, W.H. Deng, Z.J. Zheng, K.F. Yang, L.W. Xu, One-by-one hydrogenation, cross-coupling reaction, and Knoevenagel condensations catalyzed by PdCl₂ and the downstream palladium residue, *Green Chem.* 15 (2013) 2349–2355.
 - [42] K. Soai, S. Yokoyama, A. Ookawa, Reduction of azides to amines with sodium borohydride in tetrahydrofuran with dropwise addition of methanol, *Synthesis* 1 (1987) 48–49.

Update

Applied Catalysis B: Environmental

Volume 305, Issue , 15 May 2022, Page

DOI: <https://doi.org/10.1016/j.apcatb.2021.120509>



Corrigendum

Corrigendum to “A novel thiocarbamide functionalized graphene oxide supported bimetallic monodisperse Rh-Pt nanoparticles (RhPt/TC@GO NPs) for Knoevenagel condensation of aryl aldehydes together with malononitrile” [Appl. Catal. B: Environ. 225 (2018) 148–153]

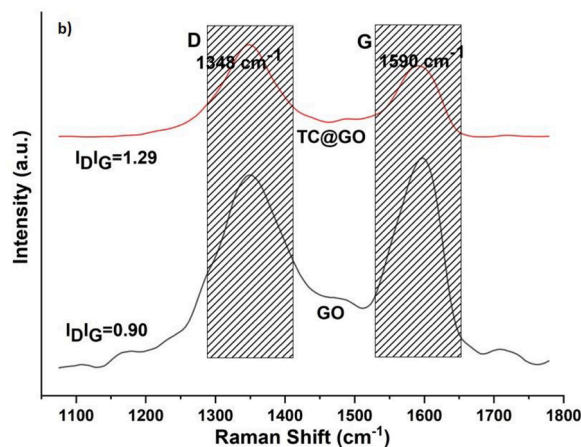
Betül Şen^{a,1}, Esmâ Hazal Akdere^{b,1}, Aysun Şavk^a, Emine Gültekin^b, Özge Paralı^a, Haydar Göksu^b, Fatih Şen^{a,*}

^a Sen Research Group, Biochemistry Department, Faculty of Arts and Science, Dumlupınar University, Evliya Çelebi Campus, 43100, Kütahya, Turkey

^b Kaynaslı Vocational College, Düzce University, Düzce, 81900, Turkey

The authors regret that Figure 1 and 2 have been published erroneously. Therefore, the authors would like to replace it with the correct one given below. In current version, the mean particle size of prepared nanoparticle is about 4.19 nm as shown in TEM image. This does not alter the discussion. The authors confirm that this change does not affect the originality and importance of the scientific findings reported in the paper. The authors would like to apologise for any inconvenience caused.

Fig. 1. (b) Raman spectra of GO and TC@GO



DOI of original article: <https://doi.org/10.1016/j.apcatb.2017.11.067>.

* Corresponding author.

E-mail address: fatihsen1980@gmail.com (F. Şen).

¹ These authors equally contributed to this work.

<https://doi.org/10.1016/j.apcatb.2021.120509>

Available online 18 October 2021

0926-3373/© 2021 Elsevier B.V. All rights reserved.

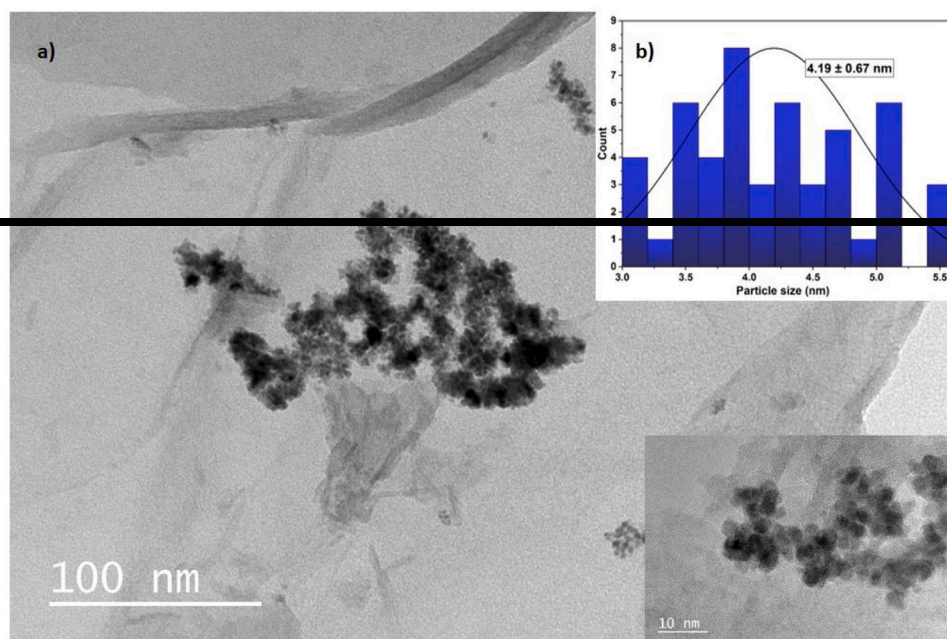


Fig. 2. (a) TEM image, (b) particle size histogram RhPt/TC@GO NPs.